

TRANSMISSION CHARACTERISTICS OF CORRUGATED ELLIPTIC GUIDE CONSIDERING HIGHER ORDER MODES IN THE SLOT REGION

T.-C. Han, F.-Y. Xu, and G.-J. Li

School of Information Science and Engineering
Lanzhou University
Lanzhou 730000, P. R. China

Abstract—Corrugated elliptic waveguide in actually extensive application is analyzed by using the mode matching method and Mathieu function. Considering space harmonics in the interior and higher order modes in the slot region of the corrugated elliptic waveguide, the dispersion equation of even TM modes is derived. The dispersion and attenuation characteristics as well as the influence of passband and stopband properties with the changes of structural parameter are investigated in detail. The calculated results in good agreement with ones in the relevant references are of very important values in theoretical studies and actual applications of corrugated elliptic waveguide for microwave engineering.

1. INTRODUCTION

The transmission of electromagnetic waves in guides with corrugated walls had been discussed and the results are interesting. Corrugated circular guide [1–3] had been studied by rayleigh-fourier method and mode matching method. Corrugated rectangular guide [4, 5] had been studied in detail. The corrugated elliptic waveguide taking no account of space harmonics was studied in 2005 [6]. The corrugated elliptic waveguide neglecting higher order modes in the slot region was studied in 2007 [7]. Corrugated waveguides play very important roles in high-power microwave tubes, corrugated antennas [8] and linear accelerators. However, the space harmonics in the interior and higher order modes in the slot region should not be ignored when analyzing corrugated elliptic waveguide in the millimeter-wave frequency range.

Considering space harmonics in the interior and higher order modes in the slot region, the characteristic equations, the passband

and stopband properties, as well as attenuation characteristic for even TM modes of the corrugated elliptic guide with finite teeth thickness are investigated in this paper. A number of important results of corrugated elliptic guide for microwave engineering are firstly obtained and verified, which is very useful in practical applications.

2. THEORETICAL ANALYSIS

2.1. Dispersion Equation

The structure of corrugated elliptic guide is shown in Fig. 1. The whole transverse cross-section is divided into two regions: region I denotes the inner elliptic space; region II denotes the corrugated area on the metal wall. ξ_1 and ξ_2 are used to describe the border of regions I and II in elliptic coordinates respectively. d and p are slot teeth separation and corrugated pitch. Assuming for all of the field components have the time dependence $e^{-j\omega t}$ throughout considering even TM modes in the corrugated elliptic waveguide.

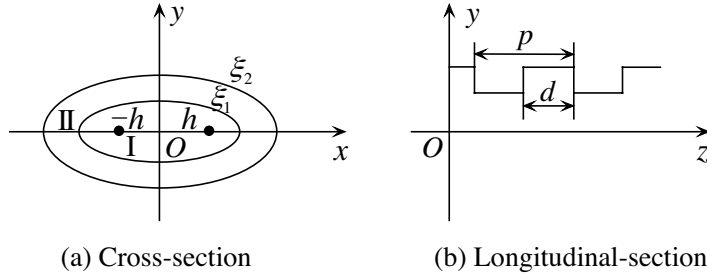


Figure 1. The cross-section of corrugated elliptic guide.

In region I, the electric field can be simply expressed as

$$E_{1z}(\xi, \eta, z) = \sum_{n=-\infty}^{\infty} A_n \text{Ce}_0(\xi, q_{1n}) \text{ce}_0(\eta, q_{1n}) e^{-j\beta_n z} \quad (1)$$

where, $\beta_n = \beta_0 + 2n\pi/p$, $k_{cn}^2 = k^2 - \beta_n^2$, $q_{1n} = h^2 k_{cn}^2/4$; $\text{ce}_0(x, q)$ and $\text{Ce}_0(x, q)$ are the zero order even Mathieu function and the zero order modified even Mathieu function of the first kind.

In region II, the electric field can be expressed as

$$E_{2z} = \sum_{l=0}^{\infty} C_l U_l^D \text{ce}_0(\eta, q_{2l}) \cos r_l z \quad (2)$$

where, $r_l = 2l\pi/d$, $w_l^2 = k^2 - r_l^2$, $q_{2l} = h^2 w_l^2/4$ and

$$U_l^D = \text{Ce}_0(\xi, q_{2l})\text{Ne}_0(\xi_2, q_{2l}) - \text{Ce}_0(\xi_2, q_{2l})\text{Ne}_0(\xi, q_{2l})$$

$\text{Ne}_0(x, q)$ is the zero order modified even Mathieu function of the second kind.

The field boundary conditions between regions I and II can be written as below

$$\left. \begin{aligned} E_{1z} &= E_{2z} & (\xi = \xi_1) \\ H_{1\eta} &= H_{2\eta} & (\xi = \xi_1) \end{aligned} \right\} \quad (3)$$

By using the orthogonality of the $\cos r_l z$ and $\sin r_l z$ over $-d/2 < z < d/2$, and the orthogonality of the $e^{-j\beta_n z}$ over $-p/2 < z < p/2$, based on Equation (3), the characteristic equation for the even TM modes of the corrugated elliptic waveguide may be gotten as

$$|\mathbf{D}_{nm}| = 0 \quad (4)$$

where,

$$\begin{aligned} \mathbf{D}_{nm} &= \begin{cases} \text{Ce}'_0(\xi_1, q_{1m})Q_{nm} - \text{Ce}_0(\xi_1, q_{1n}) & (n = m) \\ \text{Ce}'_0(\xi_1, q_{1m})Q_{nm} & (n \neq m) \end{cases} \\ Q_{nm} &= \sum_{l=0}^{\infty} \frac{w_l^2 U_l^N}{k_{cm}^2 U_l^{N'}} P_{nl}^1 P_{ml}^2 \\ P_{nl}^1 &= \frac{1}{p} \int_{-d/2}^{d/2} \cos r_l z e^{j\beta_n z} dz \\ P_{ml}^2 &= \begin{cases} \frac{1}{d} \int_{-d/2}^{d/2} e^{-j\beta_m z} dz & l = 0 \\ \frac{2}{d} \int_{-d/2}^{d/2} \cos r_l z e^{-j\beta_m z} dz & l \neq 0 \end{cases} \\ U_l^N &= \text{Ce}_0(\xi_1, q_{2l})\text{Ne}_0(\xi_2, q_{2l}) - \text{Ce}_0(\xi_2, q_{2l})\text{Ne}_0(\xi_1, q_{2l}) \\ U_l^{N'} &= \text{Ce}'_0(\xi_1, q_{2l})\text{Ne}_0(\xi_2, q_{2l}) - \text{Ce}_0(\xi_2, q_{2l})\text{Ne}'_0(\xi_1, q_{2l}) \end{aligned}$$

2.2. Attenuation

The attenuation coefficient α is given by

$$\alpha = \frac{P_L}{2P_T} \quad (5)$$

The relative attenuation coefficient $\tilde{\alpha}$ is defined as

$$\tilde{\alpha} = \sigma^{1/2} h^{3/2} \alpha \quad (6)$$

where, P_T and P_L are the transmission power and loss power per corrugation pitch respectively, P_L is then given by

$$P_L = P_{L1} + P_{L2} + P_{L3} \quad (7)$$

where, P_{L1} , P_{L2} and P_{L3} represent separately loss power on the boundary $\xi = \xi_1$, $\xi = \xi_2$ and on the sidewalls of the slot. They are given by following expression respectively

$$\begin{aligned} P_T &= \frac{p}{2} \text{Re} \left\{ \int_0^{\xi_1} \int_0^{2\pi} (E_{1\xi} H_{1\eta}^* - E_{1\eta} H_{1\xi}^*) h_1 h_2 d\eta d\xi \right\} \\ P_{L1} &= \frac{p-d}{2} R_S \int_0^{2\pi} |H_{1\eta}(\xi = \xi_1)|^2 h_2(\xi = \xi_1) d\eta \\ P_{L2} &= \frac{d}{2} R_S \int_0^{2\pi} |H_{2\eta}(\xi = \xi_2)|^2 h_2(\xi = \xi_2) d\eta \\ P_{L3} &= R_S \int_{\xi_1}^{\xi_2} \int_0^{2\pi} (|H_{2\xi}|^2 + |H_{2\eta}|^2) h_1 h_2 d\eta d\xi \\ h_1 &= h_2 = h \sqrt{\sinh^2 \xi + \sin^2 \eta} \end{aligned}$$

3. NUMERICAL ANALYSIS

By the normalized dispersion relation and solving $\omega h/c$ as a function of $\beta_0 p/\pi$, h/p , d/p , ξ_1 and ξ_2 are used to describe the dimensions of the guide.

To verify the correctness of the method in this paper, the method is firstly used to calculate elliptic guide with fixed $\xi_1 = \xi_2$ and corrugated circular waveguide with fixed $e = 0.06$. The results are compared with [9] and [10] as shown in Fig. 2 and Fig. 3. It is observed that the results of this paper are in good agreement with that of the references.

Next, the dispersion curves for the even TM modes of the corrugated elliptic guide are shown in Fig. 4. As can be seen, there are three modes such as TM_{01} , TM_{02} and TM_{03} marked by square, circle and triangle respectively. It is clearly demonstrated that $\omega h/c$ increase or decrease with $\beta_0 p/\pi$ from 0.0 to 1.0, then $\Delta(\omega h/c) = |(\omega h/c)_{\beta_0 p/\pi=1} - (\omega h/c)_{\beta_0 p/\pi=0}|$ constitutes a passband. It can be also seen there is a stopband between two arbitrary adjacent modes.

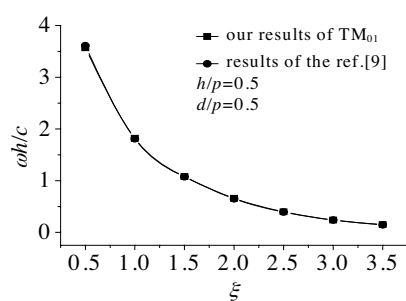


Figure 2. Calculated dispersion curve with $\xi_1 = \xi_2 = \xi$.

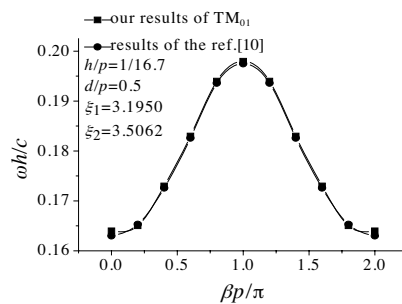


Figure 3. Calculated dispersion curve with $e = 0.06$.

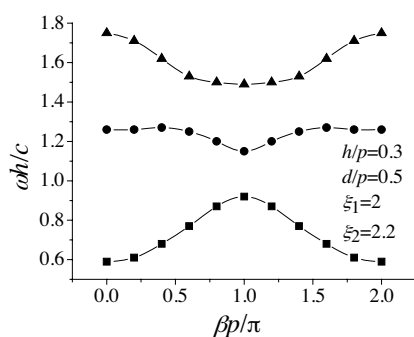


Figure 4. Dispersion curves of corrugated elliptic guide.

The results of $\omega h/c$ versus h/p , d/p and ξ_1 as $\beta_0 p = 0, \pi$ for TM₀₁ and TM₀₂ are shown in Fig. 5, Fig. 6 and Fig. 7 respectively.

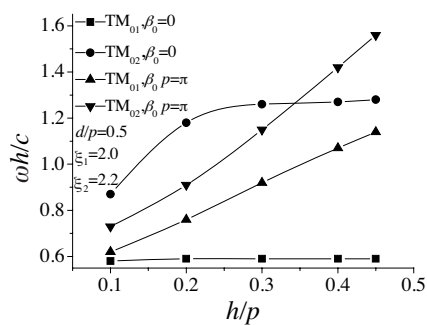


Figure 5. The relationship curves between $\omega h/c$ and h/p .

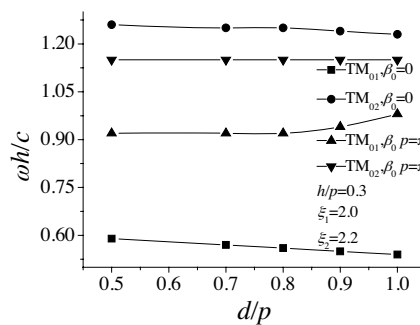


Figure 6. The relationship curves between $\omega h/c$ and d/p .

It is shown that increasing h/p can boost the passband of the waveguide and the stopband first increase then decrease with h/p in Fig. 5. It is also demonstrated that the central frequency of the stopband increases continuously with h/p .

As shown in Fig. 6, the passband and stopband are almost irrelevant to d/p . As $d/p = 1$, the proposed waveguide in this paper can be deformed into the elliptic waveguide, which can be seen as $\xi = \xi_2$. The values of $\omega h/c$ for TM_{01} , TM_{02} calculated at $\beta_0 p = 0$ are in good accord with that in [9].

Figure 7 shows that the bandwidth of the passband decreases and approximate to 0 by decreasing $\xi_1 = 1$. The passband and the central frequency of the stopband continuously increase with ξ_1 . It is demonstrated that the results of this paper are in good agreement with that of [9] at $\xi_1 = 2.2$.

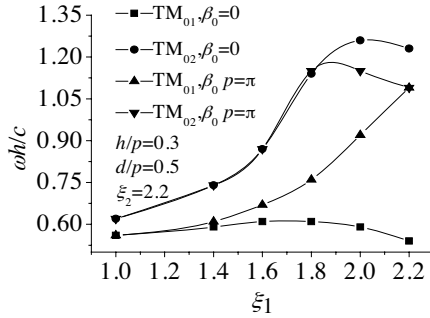


Figure 7. The relationship curves between $\omega h/c$ and ξ_1 .

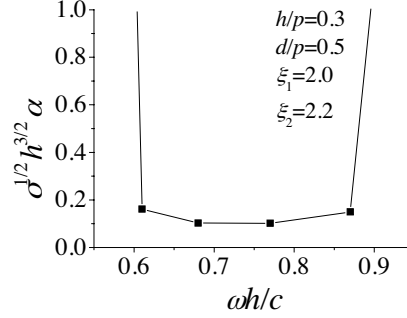


Figure 8. Attenuation coefficient $\tilde{\alpha}$ with function of $\omega h/c$.

Figure 8 shows that the relative attenuation coefficient is low in passband and increases sharply in stopband.

4. CONCLUSION

By using method of space harmonics in the interior and higher order modes in the slot region, the electromagnetic properties for even TM modes of the corrugated elliptic waveguide are investigated for the first time in this paper. It is shown that the passband and stopband are almost irrelevant to d/p . It is also demonstrated that the passband and stopband change greatly with h/p and ξ_1 . An observed important feature is that there are a series of discrete passband and stopband in the corrugated elliptic waveguide. It is also demonstrated that the relative attenuation coefficient is low in passband and increases sharply

in stopband. Numerical results in this paper provide an extension to the existing slow wave systems. The guide discussed in this paper is useful as a RF filter or a Bragg reflector.

REFERENCES

1. Barroso, J. J. and J. P. L. Neto, "Examining by the rayleigh-fourier method the cylindrical waveguide with axially rippled wall," *IEEE Transactions on Plasma Science*, Vol. 31, No. 4, 752–764, 2003.
2. Yang, H.-S. and H.-H. Yan, "The characteristic equation of corrugated circular groove guide," *International Journal of Infrared and Millimeter Waves*, Vol. 22, No. 3, 485–494, 2001.
3. Wang, S.-J. and H.-S. Yang, "The further study of corrugated circular groove waveguides by using method of space harmonics," *International Journal of Infrared and Millimeter Waves*, Vol. 23, No. 1, 485–494, 2002.
4. Epp, L. W., D. J. Hoppe, and D. T. Kelley, "A TE/TM modal solution for rectangular hard waveguides," *IEEE Transactions on Microwave Theory and Techniques*, Vol. 54, No. 3, 1048–1054, 2006.
5. Lu, Z.-G. and Y.-B. Gong, "Numerical analysis on high frequency characteristics of inner slotted rectangular waveguide grating slow-wave circuit," *High Power Laser and Particle Beams*, Vol. 18, No. 7, 1154–1158, 2006.
6. Xu, J., W.-X. Wang, and Y.-B. Gong, "Characteristic study of the periodically iris-loaded elliptical waveguide for slow-wave structures," *International Journal of Infrared and Millimeter Waves*, Vol. 26, No. 9, 1355–1368, 2005.
7. Xu, J. and W.-X. Wang, "Study of corrugated elliptical waveguides for slow-wave structures," *IEEE Transactions on Electron Devices*, Vol. 54, No. 1, 151–156, 2007.
8. Lucci, L. and R. Nesti, "Phase center optimization in profiled corrugated circular horns with parallel genetic algorithms," *Progress In Electromagnetics Research*, PIER 46, 127–142, 2004.
9. Zhang, S.-J. and Y.-C. Shen, "Eigenmode sequence for an elliptic waveguide with arbitrary eccentricity," *Acta Electronica Sinica*, Vol. 22, No. 3, 86–89, 1994.
10. Zhao, L.-X., Z.-Q. Yang, and Z. Liang, "Dispersion properties research on cylindrical slow wave structure," *The 14th Chinese Vacuum Electronics Society*, 303–306, 2003.